UNITED STATES DEPARTMENT OF THE INTERIOR

GEOLOGICAL SURVEY

Geochemical and Mineralogical Studies of a South Texas Roll Front Uranium Deposit

By

Martin B. Goldhaber and Richard L. Reynolds

Open-File Report 77-821

1977

Contents

Illustrations

Tables

Geochemical and Mineralogical Studies of a South Texas Roll Front Uranium Deposit

By Martin B. Goldhaber and Richard L. Reynolds

Abstract

Core samples from a roll-front uranium deposit in south Texas have been analyzed for iron sulfide content and mineralogy, organic carbon content and the abundance of carbonate, iron, manganese and titanium. Sulfide occurs almost exclusively as the iron disulfides pyrite and marcasite, in concentrations as high as 2 percent of the coarse (>62 μm) fraction. Marcasite is particularly abundant relative to pyrite in the vicinity of the roll front. Because marcasite precipitation requires acidic pH's and the most likely mechanism for generating a low pH is oxidation of preore sulfide, it is argued that marcasite formation is, at least in part, related to roll-front development. Organic carbon analyses from various representative parts of the deposit are uniformly low (<Ø.1 percent C). This is taken to imply that sulfate reducing bacteria were not involved in either initial sulfidation of the host rock or during later sulfidization that was related to the ore-forming episode. Carbonate minerals, such as calcite, are quite abundant, but appear to have formed after the ore. The overall abundance of iron

apparently is not systematically related to position with respect to the roll front, whereas manganese probably is concentrated near the redox interface. Titanium like iron does not show a systematic relationship to position about the roll. However, titanium is systematically more abundant in the fine fraction (<62 μm) relative to the coarse fraction with distance downdip. This reflects a progressively more intense alteration of precursor iron titanium oxide minerals to fine-grained TiO_2.

Introduction

The major reserves of uranium ore in the United States are known to occur in sedimentary rocks deposited in terrestrial or transitional marine environments (Finch, 1967). Of the major uranium producing regions, the south Texas Coastal Plain ranks third in reserves (Anonymous, 1976) and, therefore, consititutes a significant contribution to the overall domestic uranium picture. Several recent articles have reviewed the general geologic relationships of the south Texas deposits to their host rocks (Eargle and Weeks, 1973; Eargle and others, 1975; Dickinson, 1976), however, published in-depth studies of individual deposits are limited to two examples (Klohn and Pickens, 1970; Dickinson and Sullivan, 1976). This report describes the mineralogical and geochemical properties of a deposit in Webb County, Texas.

The ore host is a paleo-fluvial channel in the lower part of the Catahoula Tuff of Miocene age. In cross section the ore exhibits a C-shaped roll front as described, for example, by Adler (1974), and

Harshman (1972). Two series of core fences were drilled perpendicular to the trend of the roll front (fig. 1). The samples described below were for the most part from the southwest core fence, although some data from core 1E in the northeast fence are presented. The material studied had been disaggregated but not crushed, and stored in small paper bags.

It is important to note that the sample suite includes material from as much as 1 km on either side of the roll front. The wide sample distribution provides an excellent opportunity to examine processes occurring at some distance from ore, which may nevertheless be related to ore deposition. On the other hand, our coverage in the immediate vicinity of the roll front is somewhat more limited than that which is available by detailed sampling in a wall of an open-pit deposit. Some aspects of the heavy mineral suite in this deposit have previously been described (Granger and Warren, 1974).

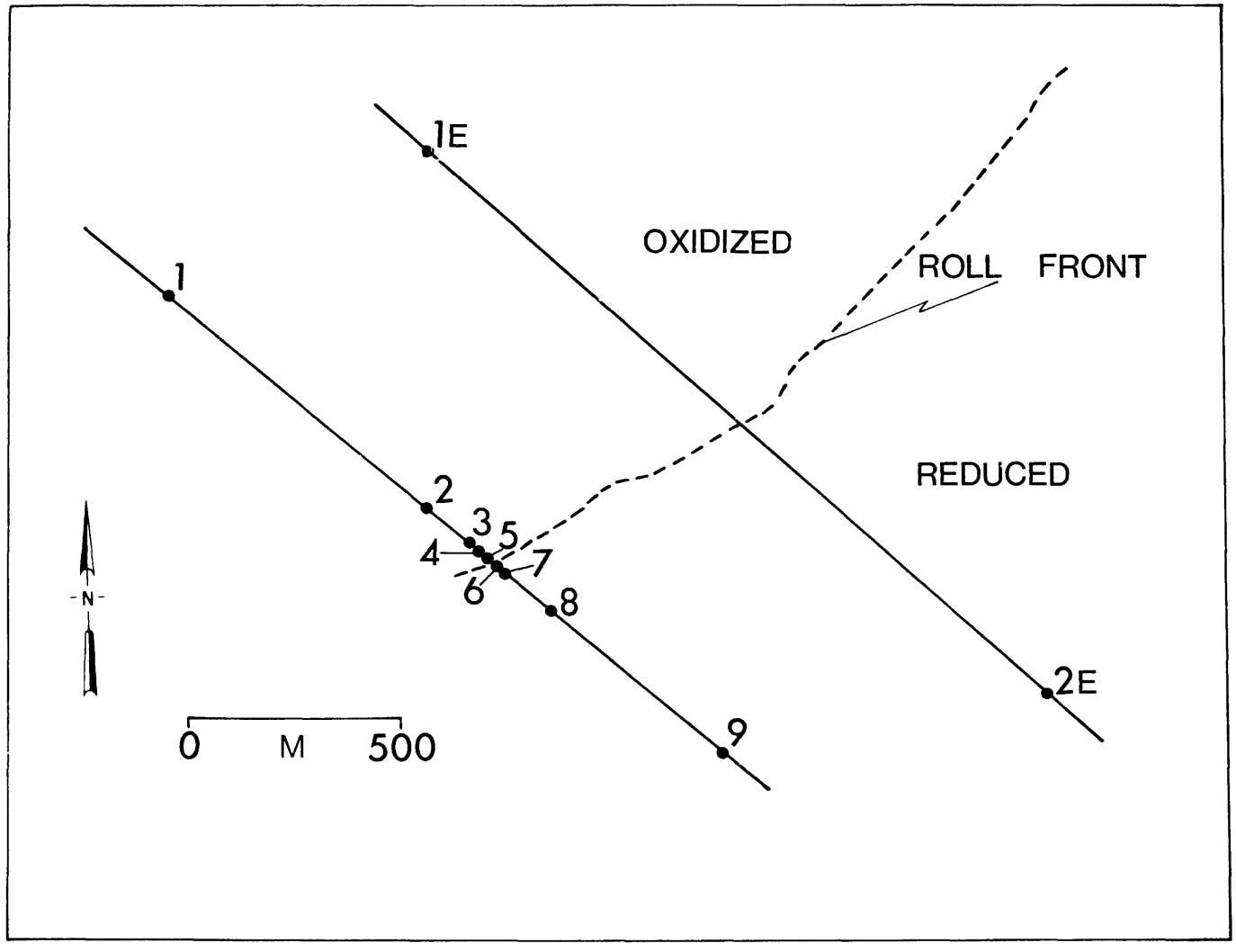

Figure 1.--Plan view of the south Texas roll front (dashed line) showing location of core holes (circles) along two fences (solid lines).

Results and Discussion

Sulfide and organic carbon content

Sulfide data were supplied to us and are reproduced with the permission of Wyoming Mineral Corp. (table 1). Figure 2 shows the weight percent of iron disulfide. In addition to the results shown, several analyses of sulfide sulfur were performed by the authors in conjunction with stable isotope studies. Our results are systematically higher, presumably because we simultaneously analyzed both coarse (>62 μm) and fine (<62 μm) fractions whereas the results shown in figure 2 refer only to the coarse fraction. The results supplied by the Wyoming Mineral Corp. display the same trends as our data but are more complete; they are, therefore, discussed preferentially. Several important features illustrated in figure 2 are worth noting. An important point is the classic roll shape defined by the interface between the absence and presence of sulfide--the redox boundary. As is typical of roll-type deposits, uranium is localized on the sulfide-bearing margin of this interface (Wyoming Mineral Corp., unpublished data). A second point to note is the existence of sulfide maxima adjacent to the redox boundary. For example, in core 4, iron sulfides are more abundant 0.6-1 m above and below the oxidation boundary than values at greater vertical distance above and below the boundary. Similar trends are displayed in cores 3 and 5. Such tends suggest that here as in other roll-type deposits, sulfide precipitation has in part been controlled by processes acting to form

Table 1.--Carbonate and iron sulfide content of core samples

[Tr., trace; leaders (---) indicates none]

Core	Depth below surface (meters)	% CO_3^{2-}	% FeS_2	Core	Depth below surface (meters)	% CO_3^{2-}	% FeS_2
1	24.7-25.3	12.6	---	3	32.0-32.9	11.8	0.18
	25.3-26.2	10.5	---		32.9-33.8	12.6	.40
	26.2-27.1	13.5			33.8-34.7	10.0	.81
	27.1-28.0	11.8	---		34.7-35.3	10.0	.49
	28.0-29.3	10			35.3-35.9	10.9	.85
	29.3-29.6	8.7	---		35.9-36.3	16.1	.44
	29.6-30.8	10.9	---		36.3-36.6	13.1	.35
	30.8-31.7	12.2	---		36.6-36.9	13.1	.50
	31.7-32.9	9.2	---		36.9-37.2	10.5	.04
	32.9-33.3	9.2	---		37.2-37.5	14.4	---
	33.3-34.4	12.6	---		37.5-37.8	14.4	---
	34.4-35.4	3.0	---		37.8-38.4	13.1	---
	35.4-36.0	7.0	---		38.4-39.0	12.2	---
	36.0-36.6	12.2	---		39.0-39.3	9.6	---
	36.6-37.8	9.6	---		39.3-39.9	13.1	---
	37.8-38.4	9.2	---		39.9-40.5	11.8	---
	38.4-39.3	12.1	---		40.5-41.1	14.0	---
	39.3-40.2	11.8	---		41.1-41.7	10.0	---
	40.2-41.4	8.7	---		41.7-42.4	11.3	---
2	30.2-30.5	10.9	0.01		42.4-43.0	9.6	---
	30.5-30.8	10.9	Tr.		43.0-43.6	14.0	---
	30.8-31.7	12.2	---		43.6-43.9	7.0	---
	31.7-32.6	10.9	---		43.9-44.2	6.5	.03
	32.6-33.8	9.2	---		44.2-44.5	9.2	Not analyzed.
	33.8-35.0	7.4	---		44.5-45.1	5.2	.59
	35.0-36.0	11.3	---		45.1-45.7	1.8	.15
	36.0-36.9	10.9	---				
	36.9-37.8	7.4	---	4	33.5-33.8	13.1	.93
	37.8-38.4	7.4	---		33.8-34.4	10.5	.39
	38.4-38.7	7.0	---		34.4-35.1	16.6	.66
	38.7-39.3	10.0	---		35.1-35.7	14.8	.48
	39.3-40.2	11.3	---		35.7-36.0	14.4	.59
	40.2-40.5	7.0	---		36.0-36.3	14.0	1.93
	40.5-41.1	9.6	---		36.3-36.6	12.2	1.30
	41.1-41.8	9.2	---		36.6-36.9	12.2	.30
	41.8-42.4	6.1	---		36.9-37.2	16.1	---
	42.4-42.7	11.8	---		37.2-37.5	9.2	---
	42.7-43.0	5.2	---		37.5-37.8	9.2	---
	43.0-43.3	12.2	.46		37.8-38.4	12.6	---
	43.3-43.6	9.2	.71		38.6-38.9	10.9	---
	43.6-43.9	10.0	.42		38.9-39.6	12.6	---
	43.9-44.2	10.9	.55		39.6-40.2	12.2	---
	44.2-44.8	11.3	.60		40.2-40.5	13.1	---
	44.8-45.4	11.8	.16		40.5-41.1	16.6	---

Table 1.--Carbonate and iron sulfide content of core samples--Continued

Core	Depth below surface (meters)	% CO_3^{2-}	% FeS_2	Core	Depth below surface (meters)	% CO_3^{2-}	% FeS_2
4 Cont.	41.1-41.4	10.0	0.12	6 cont.	37.5-37.8	8.3	0.42
	42.4-42.7	7.0	.47		37.8-38.1	9.6	.48
	42.7-43.3	7.4	.22		38.1-38.4	12.0	.26
	43.3-44.2	7.8	.31		38.4-38.7	13.0	.21
	44.2-44.8	9.6	.22		38.7-39.0	14.8	.51
					39.0-39.3	15.7	.19
5	34.1-34.4	18.3	.32		39.3-39.6	12.6	.06
	34.4-34.7	18.5	.13		39.6-40.2	16.6	.02
	34.7-35.0	12.2	.02		40.2-40.5	12.6	.04
	35.0-35.3	8.7	.12		40.5-40.8	9.6	.32
	35.3-35.6	9.6	.33		40.8-41.1	11.3	.32
	35.6-35.9	12.2	1.70		41.1-41.4	10.0	.60
	35.9-36.3	10.0	.88		41.4-41.7	14.8	.45
	36.3-36.6	10.5	.74		41.7-42.0	11.3	.34
	36.6-36.9	11.3	.70		42.0-42.4	9.6	.37
	36.9-37.2	14.0	.30		42.4-43.1	12.6	.54
	37.2-37.5	9.6	.08		43.1-43.4	10.9	.62
	37.5-37.8	9.6	---		44.2-44.8	7.8	.31
	37.8-38.1	15.3	---		44.8-45.7	8.3	.26
	38.1-38.4	14.8	---				
	38.4-38.7	12.2	---	7	33.5-34.4	9.2	.47
	38.7-39.0	9.6	---		34.4-34.7	7.0	.20
	39.0-39.3	11.8	---		34.7-35.7	11.8	.93
	39.3-39.6	9.2	---		35.7-36.3	8.3	.50
	39.6-39.9	10.9	---		36.3-37.2	13.1	.82
	39.9-40.2	14.4	---		37.2-37.8	11.8	.15
	40.2-40.5	13.5	.13		37.8-39.0	11.3	.26
	40.5-40.8	13.1	Tr.		39.0-39.6	6.5	.09
	40.8-41.1	11.8	---		39.6-40.2	11.3	.22
	41.1-41.4	10.9	---		40.2-40.6	9.2	.34
	41.4-41.7	11.3	.01		40.6-41.8	9.2	.22
	41.7-42.0	12.2	.75		41.8-42.4	9.6	.33
	42.0-42.3	11.8	.66		42.4-43.3	9.6	.36
	42.3-42.6	12.6	.78		43.3-44.2	5.2	.08
	42.6-42.9	11.8	.61	8	32.0-32.9	14.2	.73
	42.9-43.3	12.6	.58		32.9-33.8	12.1	.23
					33.8-35.1	15.3	.46
6	33.5-33.8	12.2	.48		35.1-35.7	23.1	.77
	33.8-34.4	5.7	.36		35.7-36.0	18.3	.65
	34.4-35.4	10.9	.45		36.0-36.9	19.6	.55
	35.4-36.3	12.2	.56		36.9-37.8	17.4	.23
	36.3-36.9	10.5	.68		37.8-38.4	20.9	.29
	36.9-37.5	11.3	.98		38.4-39.6	15.3	.89

Table 1.--Carbonate and iron sulfide content of core samples--Continued

Core	Depth below surface (meters)	% CO_3^{2-}	% FeS_2
8 Cont.	39.9-40.2	5.7	0.62
	40.2-41.5	11.3	.93
	41.5-42.2	10.5	1.20
	42.2-43.4	9.2	4.22
	43.4-44.7	9.2	1.44
	44.7-45.6	7.4	1.02
	45.6-46.8	7.0	.85
	46.8-48.2	12.6	.77
9	33.5-34.7	12.6	.24
	34.7-35.7	13.1	.33
	35.7-36.6	12.2	.60
	36.6-37.8	8.7	.02
	37.8-39.0	9.2	.89
	39.0-39.9	13.1	1.14
	39.9-40.8	12.6	1.72
	40.8-41.8	12.6	1.46
	41.8-42.7	11.8	.94
	42.7-43.6	13.1	.89
	43.6-44.5	13.1	1.09
	44.5-45.1	8.7	.90
	45.1-45.7	7.8	.19
	45.7-46.9	11.3	.73
	46.9-47.9	11.3	.43
	47.9-48.8	9.6	.55

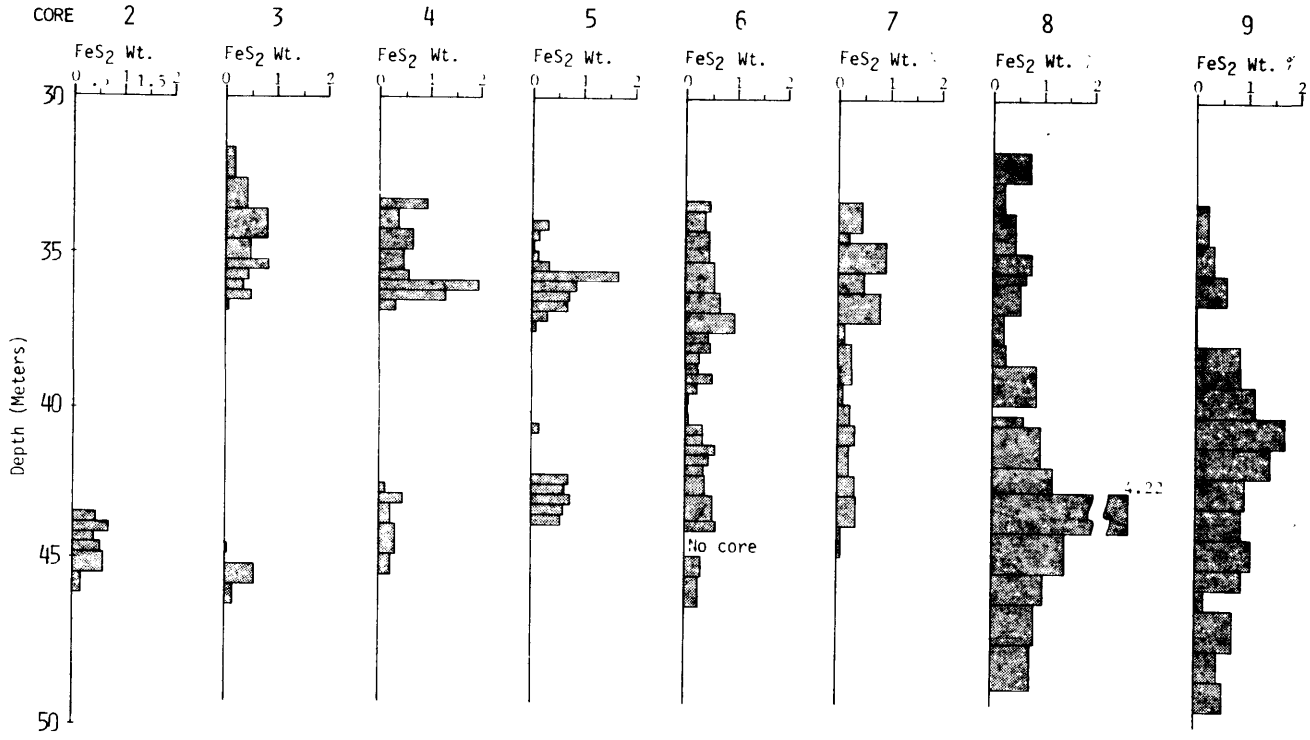

Figure 2.--Total iron sulfide as percent of the whole rock with position.

the oxidation interface (Granger and Warren, 1969; Rackley, 1972).

An exception to this relationship occurs in core 6 where sulfide is lowest adjacent to the roll. This anomaly may be related to core positioning near the nose of the roll. Higher values would presumably have been observed had the core been taken about half a meter further downdip.

Organic carbon analyses were performed using the LECO^{R} induction furnace technique. Carbonate carbon was removed in a preliminary step using dilute hydrochloric acid. Analyses were carried out in duplicate and are summarized in table 2. The samples chosen span the range of geochemical environments present in the deposit (oxidized rock remote from ore, oxidized tongue, ore, and reduced rock downdip from ore). In few of the analyses does the organic carbon content significantly exceed the analytical detection limit of 0.01 percent C. These results are similar to those obtained by Harshman (1974) from a deposit in Live Oak County, Texas. They strongly suggest to us that oxidative degradation of organic matter by heterotrophic micro-organisms (bacteria) could not have occurred to any major extent in this deposit. In particular, sulfate reducing bacteria are excluded from playing a genetic role, as they require an organic carbon substrate (Goldhaber and Kaplan, 1974). This is illustrated by way of a schematic equation for bacterial sulfate reduction in which organic matter is assumed to have the oxidation state of carbohydrate:

$$2(CH_2O)+SO_4^{2-} \longrightarrow 2HCO_3^- + H_2S. \qquad (1)$$

In contrast to the low organic carbon levels the iron disulfide abun-

Table 2.--Results of organic carbon analyses.

[Analysis by G. Claypool, U.S. Geological Survey.

Leaders (---) indicate not detected]

Core	Run 1	Run 2	Geochemical environment
1	---	---	Oxidized, remote from roll.
2	---	---	Oxidized tongue.
3	---	---	Oxidized tongue.
	0.01	0.12	Lower limb, in ore.
4	---	---	Lower limb, in ore.
6	.07	.07	Reduced.
	---	.06	Reduced, in ore.
	.16	---	Reduced.
8	.09	.07	Reduced.
	.06	.03	Reduced.
9	.05	---	Reduced, remote from roll.

dances are quite high, as much as 2 percent of the coarse fraction. Based upon results from marine sediments, had the sulfide been biogenic, one would have expected residual organic carbon contents remaining after sulfate reduction to be above 5 percent (Berner, 1970; Sweeney, 1972; Goldhaber and Kaplan, 1974). The lack of significant organic carbon does not preclude an important role for autotrophic micro-organisms such as those which oxidize pyrite. The low levels of organic carbon also suggest that organic matter could not have played an important role in processes related to ore localization such as reduction or adsorption of the uranyl ion.

Sulfide mineralogy

Reflected-light microscopic examination was made of numerous polished sections prepared from the heavy minerals (separated in bromoform) of the coarse-grained fractions (>62 μm). Sulfides observed are exclusively pyrite (cubic FeS_2) and marcasite (orthorhombic FeS_2).

X-ray techniques were then employed to produce semiquantitative estimates of the relative abundances of these phases. The heavy mineral fraction was treated with HCl to remove both carbonate and iron oxides and then hydrofluroic acid to decompose silicates (Neuerburg, 1975). The residue from this treatment was scanned using CuK-α radiation from 20° to $68^{\circ} 2\theta$. With only rare exceptions, all peaks could be assigned to pyrite or marcasite. A ratio, R, was formed the intensity of the marcasite peak (M) at $51.9^{\circ} 2\theta$ to the sum of M and the intensity of the pyrite peak (P) at $47.4^{\circ} 2\theta$ as follows:

$$R = \frac{M(51.9)}{M(51.9)+P(47.4)}. \qquad (2)$$

These ratios are given in table 3. For comparative purposes the largest value (R = Ø.68) corresponds to approximately 95-98 percent marcasite whereas the minimum, R = Ø.Ø2 to about 3-5 percent marcasite. Clearly marcasite is an extremely important phase in this deposit. Figure 3 is a plot of the average values of the ratio (equation 2) as a function of relative position in the deposit (vertical bars represent the observed range). These average values increase systematically from the downdip to the updip direction. The single exception is in samples from core 2 which contain relatively little marcasite (low R).

Pyrite and marcasite have both been synthesized in the laboratory at low temperatures (<1ØØ°C). The major influence on which of the two sulfides forms is thought to be pH; low pH(5.5 or less) is required for precipitation of synthetic marcasite (Rickard, 1969). If this is the case in the deposit then the increase in marcasite near the roll front may indicate that this sulfide is related to an episode of acidic pH values at some time during the history of the deposit. One likely mechanism for producing acid solutions is the oxidation of pyrite as given in equation (3):

$$4FeS_2+15Ø_2+14H_2O \longrightarrow 4Fe(OH)_3+16H^+ + 8SO_4^{2-}. \qquad (3)$$

This line of reasoning links marcasite formation to the development of the oxidized tongue and therefore presumably to the time of ore placement. Petrographic observations of sulfides from near the roll

Table 3.--Relative ratio of marcasite to total sulfide.

[C. Gent, analyst. Column R is product of equation 2; leaders (---) indicate no estimate]

Core	Depth, meters	R*	Visual estimate of percent marcasite
2	43.0-43.6	0.01	---
	43.6-44.8	.02	---
3	32. -34.7	.64	---
	35.3-36.9	.61	---
	43.9-45.1	.61	---
4	33.5-33.8	.39	---
	33.8-34.4	.47	---
	34.4-35.1	.61	---
	35.1-35.7	.51	---
	35.7-36.0	.43	---
	36.0-36.3	.59	---
	36.3-36.6	.66	---
	36.6-36.9	.63	---
	41.1-41.4	.59	---
	42.4-42.7	.57	---
	42.7-43.3	.51	---
	43.3-44.2	.56	---
	44.2-44.8	.68	95-99
6	34.4-37.8	.44	---
	37.8-38.1	.63	---
	38.1-39.3	.56	---
	39.3-41.1	.47	---
	41.1-42.0	.49	---
	42.0-43.4	.49	---
8	32. -36.9	.08	---
	36.9-38.4	.23	---
	38.4-39.6	.37	---
	42.2-43.4	.44	---
	43.4-48.2	.38	---
9	39. -44.5	.02	10
	44.5-45.7	.33	40
	45.7-48.8	.37	45

*See equation (2).

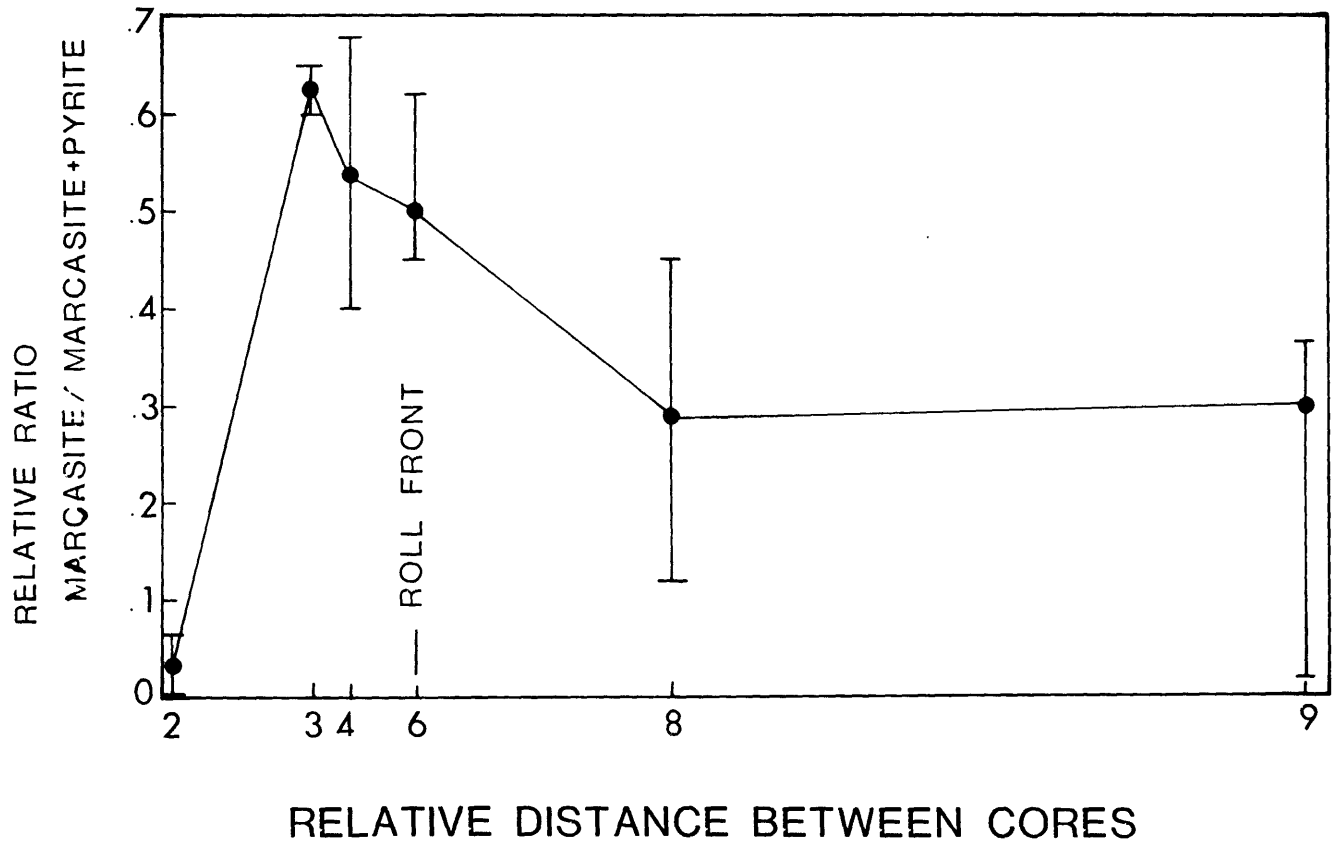

Figure 3.--Plot of the relative abundance of marcasite to total sulfide as a position of core location.

front are consistent with the idea that marcasite represents a paragenetically distinct episode, in that it is frequently observed as rims on pyrite (Goldhaber and Reynolds, unpub. data), and with the increased relative abundance of marcasite adjacent to and immediately downdip from the roll front (fig. 3).

Carbonate abundance

Weight percent carbonate (expressed as CO_3^{2-}) was determined by, and data are presented with permission of Wyoming Mineral Corp. (table 1). We independently made similar analyses on a limited suite of samples in conjunction with stable isotope studies on carbonates, and our data are in good agreement with those in table 1. Preliminary exmination of thin sections demonstrates that the carbonate being analyzed is essentially pure calcite. Plots of the abundance data (not shown) suggest that there is some weak relationship between sample position with respect to the redox interface and carbonate abundance. There appears to be a greater abundance of calcite at the nose of the roll (core 6), continuing for some distance downdip into core 8 than elsewhere. Calcite is most plentiful in core 8. Moreover, there are some minor but noticeable shifts in carbonate abundance vertically across the redox boundary in core 4. Other than these characteristics, the overall aspect of the data is essentially constant cabonate content for all samples. This is in contrast to the roll-type deposits in Wyoming where carbonate is typically absent in the oxidized tongue but locally present as cement in reduced ground ahead of the roll (Harshman, 1972). There are at least two explanations for the distribution of carbonate we observed: (1)

Calcite present today was about the same as at the time of roll formation. Local redistribution took place during pyrite oxidation as a result of hydrogen ion generation leading to some enrichment downdip as these solutions were progressively neutralized. (2) Carbonate was originally much less abundant prior to and during ore emplacement than at present. Subsequently, calcium and bicarbonate ions were introduced by ground waters so that carbonate precipitation was in part controlled or modified by the extant redox interface. We favor the latter hypothesis. The primary evidence is petrographic; carbonate appears to be everywhere paragenetically later than sulfide and ore-bearing phases. Secondly, had the high carbonate content been present during ore genesis, it is unlikely that the pH of the ground water could have dropped low enough for extensive marcasite formation.

Whereas the bulk of the calcite is present as cement in the Catahoula, some subordinate amount of carbonate was typically deposited with sands as carbonate rock fragments (McBride and others, 1968), and the samples studied herein are no exception, judging from the presence of rare microfossils in thin section.

Chemical analysis

A group of samples representing the geochemically distinguishable portions of the deposit was separated into a coarse (>62 μm) and fine fraction and was submitted for analysis of Fe, Ti, and Mn by X-ray flourescence. The analytical results are summarized in tables 4, 5, and 6. Data are reported as percent by weight of the sample. The Fe and Ti results are also recalculated to a carbonate free basis (CFB). The rationale for considering the analyses on a CFB is that if, as appears to be the case, the calcite is paragenetically late, it could simply act as a dilutant and obscure trends established during the ore-forming episode. This is probably the case for Fe and Ti although the Mn distribution seems to be in part directly related to carbonate content (see following). Bulk carbonate analyses have been utilized in making the recalculation of CFB. This is probably a good approximation for the coarse fraction which makes up the majority of he bulk sample. However, the carbonate content of the fines could differ significantly from the total sample. Based upon X-ray analysis of this sample suite (Goldhaber and others, unpub. data), it is likely that calcite content in the fines is relatively greater than the overall sample and the CFB results of the fines would therefore be an underestimate.

The iron analyses are plotted on a CFB in figure 4. All analyses in each core were averaged. Cores 2 and 3 penetrated the oxidized tongue and therefore contain both oxidized and reduced rock. Segregating the data in these two cores into oxidized and reduced

Table 4.--Iron analyses of samples representing geochemically distinguishable parts of the deposit.

[Analyst, Leon Groves. N.D., no data]

Core	Depth below surface, meters	% Fe_{coarse}	% Fe_{fines}	% Fe_c (CFB)*	%Fe_f (CFB)
1	28 -32.9	2.1	3.9	2.5	4.5
1E	34.1-40.2	2.3	2.9	2.8	3.5
	40.2-42.7	2.2	3.8	2.7	4.6
	42.7-44.2	3.6	3.0	4.4	3.7
2	30.5-35.1	1.9	3.9	2.3	4.7
	35.1-37.8	2.3	3.9	2.8	4.7
	38.7-41.1	2.1	4.1	2.5	4.9
	41.8-43	3.6	5.1	4.1	5.9
	43 -43.6	2.6	3.3	3.1	4.0
	43.6-44.8	2.3	3.3	2.8	4.0
3	32.0-34.7	2.0	2.9	2.5	3.6
	35.4-36.6	1.9	3.1	2.4	4.0
	36.9-38.1	2.2	4.5	2.9	5.9
	38.1-42.4	2.4	4.3	3.0	5.3
	42.4-43.9	3.5	4.4	4.2	5.3
	43.9-45.1	3.5	4.4	4.0	5.0
4	33.2-33.5	N.D.	3.3	N.D.	4.2
	33.5-34.1	N.D.	3.8	N.D.	4.6
	34.1-34.7	N.D.	3.1	N.D.	4.3
	34.7-35.7	N.D.	2.8	N.D.	3.7
	35.7-36.0	N.D.	3.0	N.D.	3.9
	36.0-36.3	N.D.	3.5	N.D.	4.5
	36.3-36.6	N.D.	3.3	N.D.	4.2
	36.6-36.9	N.D.	3.3	N.D.	4.1
	37.5-39.5	N.D.	4.0	N.D.	4.9
	42.1-42.4	N.D.	3.8	N.D.	4.5
		N.D.	4.2	N.D.	4.8
	42.4-42.7	N.D.	3.1	N.D.	3.6
	42.7-43.3	N.D.	4.1	N.D.	4.7
	43.3-44.2	N.D.	3.9	N.D.	4.6
	44.2-44.8	N.D.			

Table 4.--Iron analyses of samples--continued

Core	Depth below surface, meters	% Fe_{coarse}	% Fe_{fines}	% Fe_c (CFB)*	% Fe_f (CFB)
6	34.4-36.9	2.5	3.5	3.0	4.3
	36.9-38.1	2.8	3.4	3.4	4.0
	38.1-39.3	1.7	2.6	2.1	3.4
	39.3-40.8	2.1	2.8	2.6	3.8
	40.8-41.8	2.1	2.3	2.6	2.9
	41.8-42.4	1.8	3.1	2.2	3.8
8	32.0-36.9	1.8	2.9	2.5	4.0
	36.9-38.4	1.7	2.5	2.6	3.7
	38.4-39.3	1.8	2.6	2.4	3.5
	42.1-44.5	2.1	3.4	2.5	4.0
	44.5-47.9	2.3	3.4	2.7	4.0
9	39.3-44.2	1.9	2.9	2.4	3.7
	44.2-45.8	3.3	3.8	3.8	4.4
	45.8-48.8	2.2	3.0	2.7	3.7

* Carbonate free basis.

Table 5.--Manganese analyses of samples representing geochemically distinguishable parts of the deposit.

[Analyst, Leon Groves. N.D., no data]

Core	Depth below surface, meters	% Mn_{coarse}	% Mn_{fines}	%$CaCO_3$
1	28 -32.9	0.07	0.09	17.5
1E	34.1-40.2	.10	.14	
	40.2-42.7	.09	.12	
	42.7-44.2	.11	.13	
2	30.5-35.1	.07	.11	16.7
	35.1-37.8	.09	.16	16.6
	38.7-41.1	.08	.14	15.9
	41.8-43	.07	.09	12.9
	43 -43.6	.08	.10	17.8
	43.6-44.8	.04	.09	18.0
3	32 -34.7	.09	.13	19.3
	35.4-36.6	.09	.14	22.3
	36.9-38.1	.09	.15	23.5
	38.1-42.4	.08	.16	19.7
	42.4-43.9	.07	.10	17.1
	43.9-45.1	.04	.06	12.7
4	33.2-33.5	N.D.	.12	21.9
	33.5-34.1	N.D.	.08	17.5
	34.1-34.7	N.D.	.12	27.7
	34.7-35.7	N.D.	.12	24.7
	35.7-36.0	N.D.	.13	24.0
	36.0-36.3	N.D.	.12	23.4
	36.3-36.6	N.D.	.11	20.4
	36.6-36.9	N.D.	.13	20.3
	37.5-39.5	N.D.	.12	18.9
	42.1-42.4	N.D.	.10	16.8
	42.4-42.7	N.D.	.06	11.7
	42.7-43.3	N.D.	.07	12.3
	43.3-44.2	N.D.	.05	13.0
	44.2-44.8	N.D.	.06	16.0

Table 5.--Manganese analyses--Cont.

Core	Depth below surface, meters	% Mn_{coarse}	% Mn_{fines}	% $CaCO_3$
6	34.4-36.9	.09	.13	18.7
	36.9-38.1	.08	.16	16.3
	38.1-39.3	.10	.19	23.2
	39.3-40.8	.10	.17	20.9
	40.8-41.8	.11	.17	20.1
	41.8-42.4	.08	.16	18.4
8	32.0-36.9	0.09	0.11	28.7
	36.9-38.4	.11	.12	32.1
	38.4-39.3	.09	.14	25.7
	42.1-44.5	.07	.11	15.1
	44.5-47.9	.07	.11	15.1
9	39.3-44.2	.07	.13	21.2
	44.2-45.8	.05	.07	13.8
	45.8-48.8	.04	.10	17.9

Table 6.--Titanium analyses of samples representing geochemically distinguishable parts of the deposit.

[Analyst, Leon Groves]

Core	Depth below surface, meters	% Ti_{coarse}	% Ti_{fines}	% Ti_c (CFB)*	%Ti_f (CFB)*
	28.0-32.9	0.27	0.24	0.33	0.29
	34.1-40.2	.27	.26	.33	.32
	40.2-42.7	.24	.16	.29	.20
	42.7-44.2	.35	.25	.43	.30
	30.5-35.1	.38	.28	.46	.34
	35.1-37.8	.40	.35	.48	.42
	38.7-41.1	.41	.43	.49	.51
	41.8-43.0	.30	.27	.34	.31
	43.0-43.6	.32	.33	.38	.40
	43.6-44.8	.32	.34	.39	.41
	32.0-34.7	.32	.34	.40	.42
	35.4-36.6	.26	.37	.33	.48
	36.9-38.1	.46	.44	.60	.58
	38.1-42.4	.28	.32	.34	.40
	42.4-43.9	.33	.32	.40	.39
	43.9-45.1	.28	.25	.32	.29
	34.4-36.9	.27	.48	.33	.58
	36.9-38.1	.30	.44	.35	.53
	38.1-39.3	.23	.31	.30	.41
	39.3-40.8	.23	.26	.29	.32
	40.8-41.8	.22	.30	.28	.38
	41.8-42.4	.31	.52	.38	.64
	32.0-36.9	.35	.35	.49	.49
	36.9-38.4	.20	.14	.30	.21
	38.4-39.3	.26	.28	.35	.38
	42.1-44.5	.32	.50	.38	.59
	44.5-47.9	.31	.32	.37	.38
	39.3-44.2	.40	.44	.51	.56
	44.2-45.8	.29	.32	.34	.37
	45.8-48.8	.29	.42	.35	.57

* Carbonate free basis.

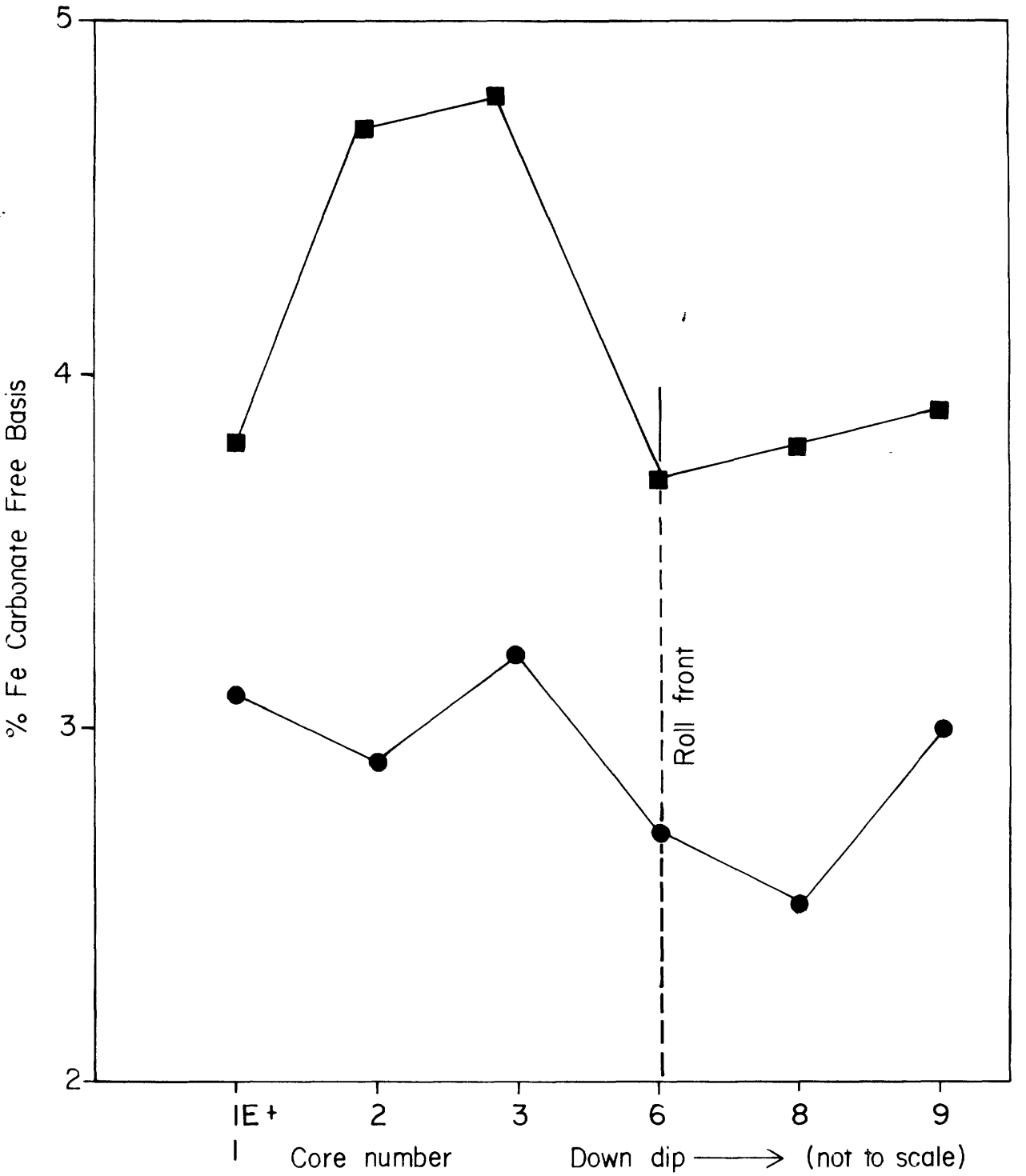

Figure 4.--Average iron abundance as a function of core location. Results are expressed as a percent by weight of the carbonate free bulk sample: ■ less than 62 micrometer size fraction; ○ greater than 62 micrometer size fraction.

facies does not qualitatively alter the trends in figure 4. Several features in the data are worth noting. Iron is concentrated, on a relative basis, in the fine fraction. This enrichment is fairly constant throughout the deposit although there is a suggestion that it is somewhat more pronounced in cores 2 and 3. Iron in many sediments shows a positive correlation with clay content because it commonly occurs as a structural component in clays as well as in iron oxide coatings on clay surfaces (Carrol, 1958). In the present context, it is reasonable to suppose that iron was concentrated in the clay fraction during either pre- or post-ore argillization of volcanic rock fragments and possibly shards(?) to montmorillonite. Of course, numerous other geochemical processes operated in these sediments. For example, the additional relative iron concentrations in the fine fraction in cores 2 and 3 might have resulted from the oxidation of sulfidized iron-bearing phases such as Fe-Ti oxides and sulfide cement provided that some of the products of sulfide oxidation occur as fine-grained iron oxides. Additional iron may have been released by oxidation of other metastable Fe-bearing silicates such as biotite.

Of interest is the fact that iron is as concentrated, and perhaps even enriched on the updip, oxidized side of the deposit compared to the downdip (reduced) portion. It has frequently been reported from other deposits (including one from nearby Live Oak County) that iron is concentrated on the downdip side of the roll (Harshman, 1974). Such distributions are taken to indicate iron mobility from the oxidized tongue into reduced rock during ore

genesis. Note that the previously reported distributions are within a few tens of meters on either side of a redox interface. Our horizontal sampling may not be sufficiently dense to observe such variations. Vertically, however, our control is excellent and iron is, if anything, higher in the oxidized tongue (for example, cores 3, 4) than above and below. These data are difficult to reconcile with the presumed generation of hydrogen ions during pyrite oxidation (equation 3) and, as noted above, the presence of ore stage marcasite (which requires an acidic environment for formation). In general, iron solubility and therefore the likelihood of iron transport increases with decreasing pH. One might therefore predict an iron distribution in this deposit similar to those previously observed. There is, in fact, observational evidence that iron was in part conserved in a solid phase during sulfide oxidation. Iron oxide and iron oxyhydroxide pseudomorphs after pyrite are commonly observed in the oxidized tongue (Reynolds and Goldhaber, 1977). Further work is necessary to reconcile these inconsistencies in the geochemistry of iron.

Manganese data are reported in table 6. These data indicate that as for Fe, manganese is concentrated in the fine fraction. In contrast to the Fe distribution, however, manganese may bear a more conspicuous relationship to position in the deposit. The highest Mn values are in ore near the nose of the roll (core 6). Preliminary microprobe analysis of individual uranium-bearing grains from core 6 do indicate the occasional presence of manganese. However, a major control on manganese is related to carbonate geochemistry, as

suggested by the positive correlation between bulk carbonate and manganese in both the fine (fig. 5) and coarse (fig. 6) fraction. It seems reasonable to suppose that manganese was available in solution during carbonate precipitation and was either trapped by coprecipitation in the carbonate (Raiswell and Brimblecombe, 1977) or perhaps present a a discrete manganese carbonate phase in abundance below the detection limit of the X-ray analyses. This association between manganese and mineral carbon has previously been noted from roll-front deposits in the Shirley Basin, Wyoming (Harshman, 1976).

If our inference is correct that calcite precipitation was paragenetically later than roll front development, it follows that (with the possible exception of core 6) major control on the observed manganese distribution was not related to ore-forming processes.

Titanium analyses are contained in table 6 and averaged values are plotted on figure 7 (CFB). The most striking trend is that Ti in the fine fraction increases in the downdip direction. Furthermore, updip samples from cores 1E + 1 and 2 show higher percentages of Ti in the coarse fraction. This relationship reversed with distance downdip such that, in the remaining cores, Ti is more abundant in the fine fraction. Based upon petrographic studies presented elsewhere (Reynolds and Goldhaber, unpub. data), we have established that intensity of sulfidization increases downdip and is related to the presence of a fault located downdip from 9 which released hydrogen sulfide to the host sands. The Ti data may be rationalized on the basis of transfer of Ti from detrital grains such as titanohematite and titanomagnetite in the coarse fraction to TiO_2 (anatase) in the

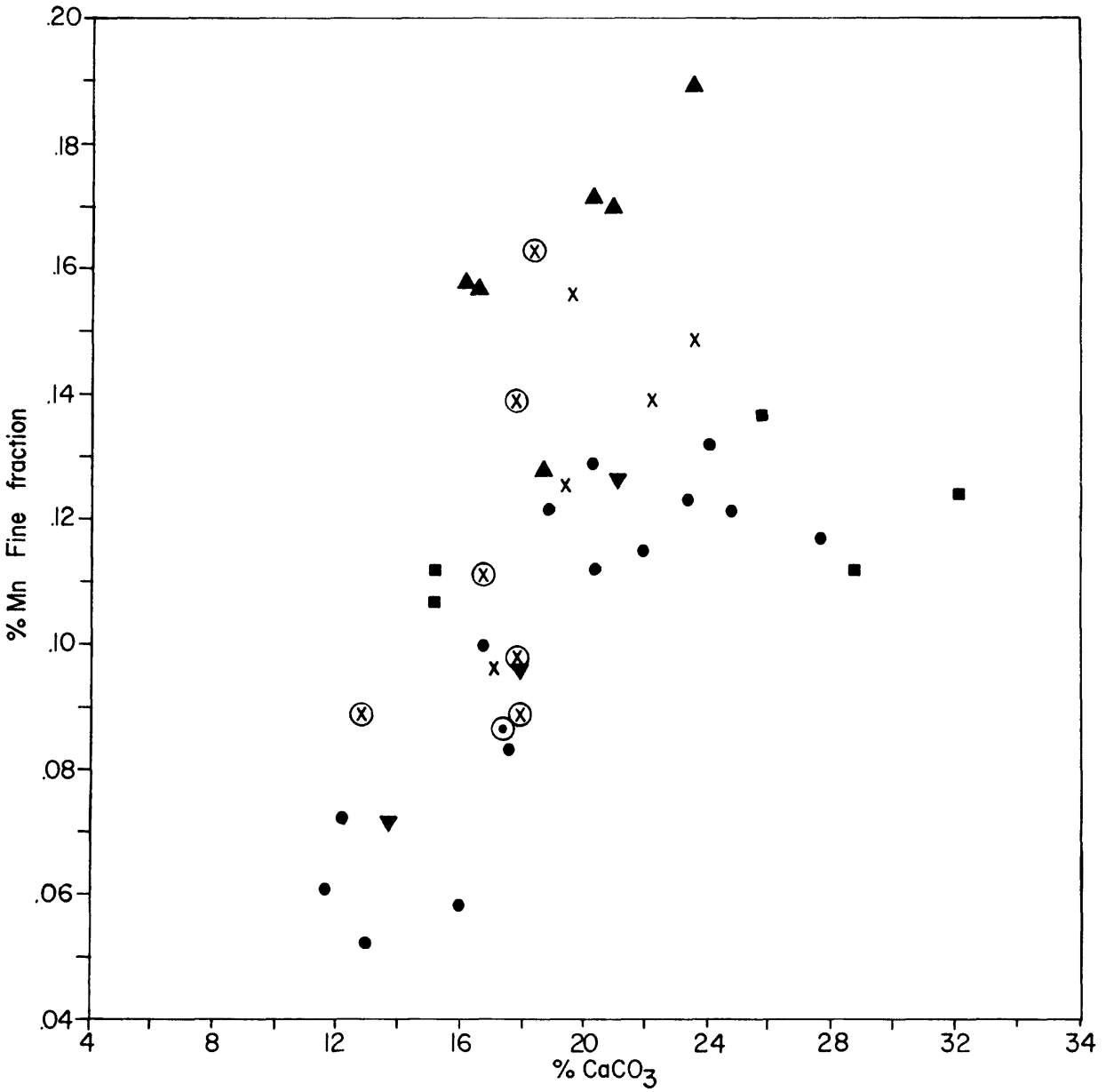

Figure 5.--Plot of weight percent manganese in the less than 62 micrometer fraction against abundance of calcium carbonate: ◯ core 1, ⊗ core 2, X core 3, ● core 4, ▲ core 6, ■ core 8, ▼ core 9.

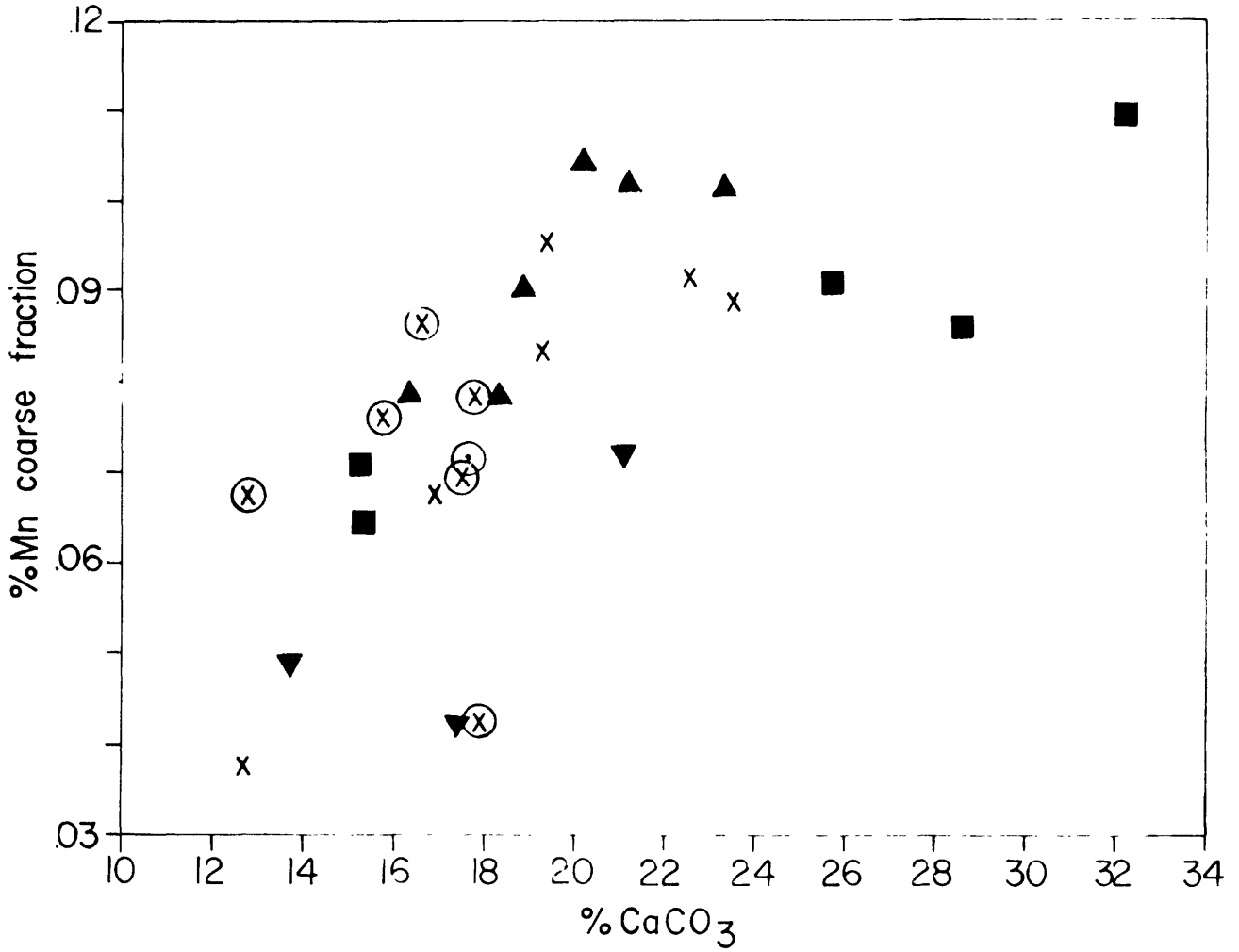

Figure 6.--Plot of weight percent manganese against carbonate content. Symbols represent ⊙ core 1, ⊗ core 2, X core 3, ▲ core 6, ■ core 8, ▼ core 9.

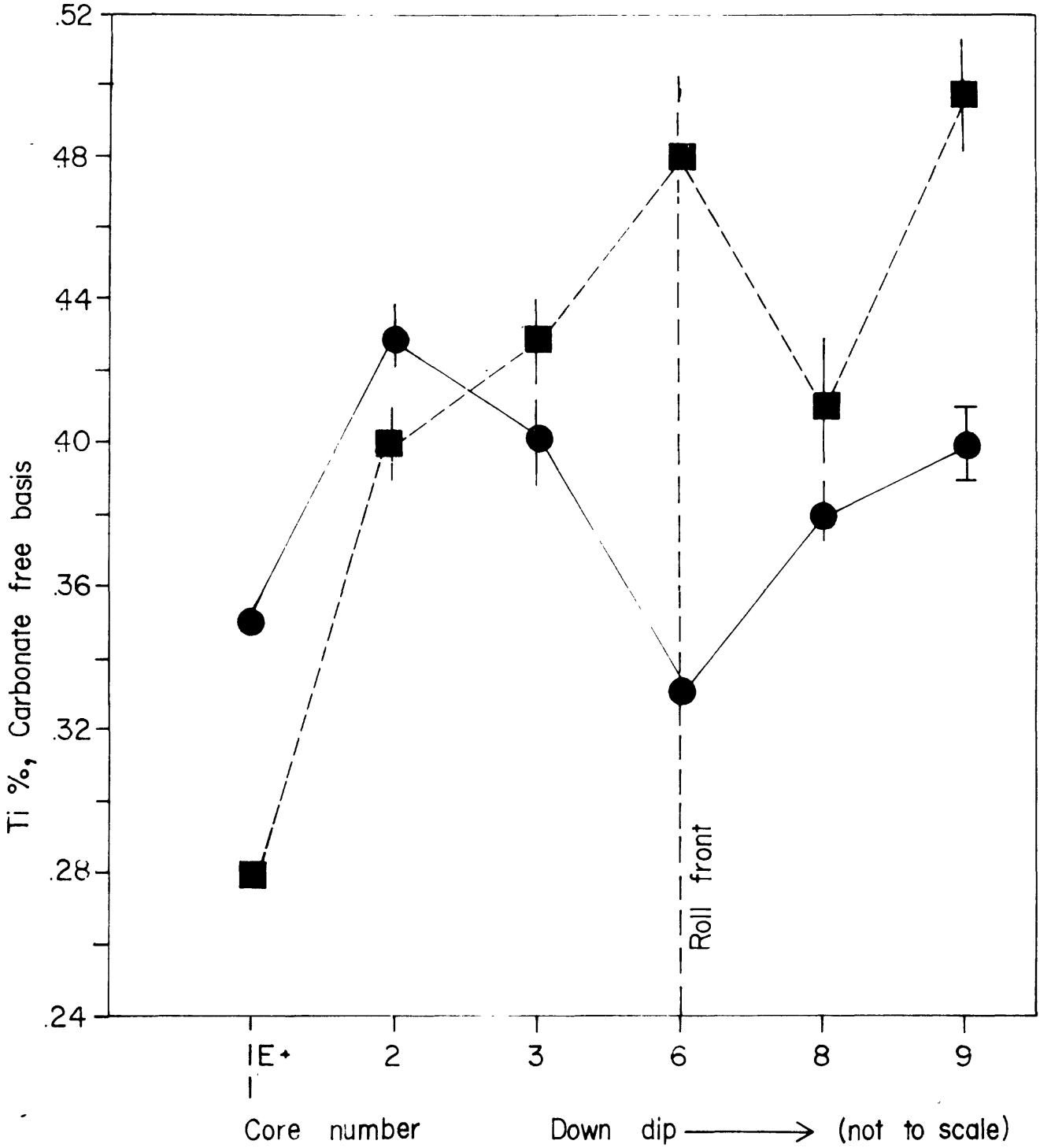

Figure 7.--Plot of titanium averaged content of core samples expressed as a weight percent of the carbonate free bulk sample against core position relative to the roll front (not to scale); ● greater than 62 micrometer size fraction, ■ less than 62 micrometer size fraction.

fines by reactions of the type (Adams and others, 1974).

$$FeTiO_3 + 2H_2S \longrightarrow TiO_2 + FeS + H_2O \quad . \qquad (4)$$

Because sulfidization was more intense downdip (closer to the fault) reactions such as (4) went on to a greater extent in core 9 leading to the highest content of Ti in the fine fraction.

References Cited

Adams, S. S., Curtis, H. S., and Hafen, P. L., 1974, Alteration of detrital magnetite ilmenite in continental sandstones of the Morrison Formation, New Mexico, in Formation of uranium deposits: Internat. Atomic Energy Agency, Proc., Vienna, p. 219-253.

Adler, H. H., 1974, Concepts of Uranium ore formation in reducing environments in sandstones and other sediments, in Formation of uranium ore deposits: Internat. Atomic Energy Agency, Proc., Vienna, p. 141-168.

Anonymous, 1976, National uranium resource evaluation--preliminary report: U.S. Research and Develop. Admin. GJO-111(76), 132 p.

Berner, R. S., 1970, Sedimentary pyrite formation: Am. Jour. Sci., v. 268, p. 1-23.

Carroll, D., 1958, Role of caly minerals in the transportation of iron: Geochim. et Cosmochim. Acta, v. 14, p. 1-27.

Dickinson, K. A., 1976, Sedimentary depositional environments of uranium and petroleum host rocks in the Jackson Group, south Texas: U.S. Geol. Survey Jour. Research, v. 4, p. 615-629.

Dickinson, K. A., and Sullivan, M. W., 1976, Geology of the Brysch uranium mine, Karnes County, Texas: U.S. Geol. Survey Jour. Research, v. 4, p. 397-404.

Eargle, D. H., and Weeks, A. M. D., 1973, Geologic relations among uranium deposits, south Texas coastal plain region, USA, in Amstutz, C. G., and Bernard A. J., eds., Ores in sediments: New York, Springer-Verlag, PIOI-113.

Eargle, D. H., Dickinson, K. A., and Davis, B. O., 1975, South Texas uranium deposits: Am. Assoc. Petroleum Geologists Bull., v. 59, p. 766-779.

Finch, W. I., 1967, Geology of epigenetic uranium deposits in sandstone in the United States: U.S. Geol. Survey Prof. Paper 538, 121 p.

Goldhaber, M. B., and Kaplan, I. R., 1974, The sulfur cycle, in Goldberg, E. O., ed., The Sea, v. 5, Marine Chemistry: New York, John Wiley and Sons, p. 569-655.

Granger, H. C., and Warren, C. G., 1969, Unstable sulfur compounds and the origin of roll-type uranium deposits: Econ. Geology, v. 64, p. 160-171.

_____1974, Zoning in the altered tongue associated with roll-type urnium deposits, in Formation of uranium ore deposits: Internat. Atomic Energy Agency, Proc., Vienna, p. 185-200.

Harshman, E. N., 1972, Geology and uranium deposits, Shirley Basin area: U.S. Geol. Survey Prof. Paper 745.

_____1974, Distribution of elements in some roll-type uranium deposits, in Formation of uranium ore deposits: Internat. Atomic Energy Agency, Proc., Vienna, p. 169-183.

Klohn, M. L., and Pickens, W. R., 1970, Geology of the Felder uranium deposit, Live Oak County, Texas; paper presented at AIME annual mtg., Denver, Colo., Feb. 15-19, 1970: Mining Engineer Preprint no. 70-1-38, 19 p.

McBride, E. F., Lindemann, W. L., and Freeman, P. S., 1968, Lithology and petrology of the Gueydan (Catahoula) Formation in south Texas: Texas Univ. Bur. Econ. Geology Rept. Inv. 67.

Neuerburg, G. J., 1975, A procedure using hydrofluoric acid, for quantitative mineral separations from silicate rocks: U.S. Geol. Survey Jour. Research, v. 3, p. 377-378.

Rackley, R. I., 1972, Environment of Wyoming Tertiary uranium deposits: Am. Assoc. Petroleum Geologists Bull., v. 56, p. 755-744.

Raiswell, R., and Brimblecombe, P., 1977, The partition of manganese into aragonite between 30° and 60°C: Chem. Geology, v. 19, p. 145-151.

Reynolds, R. L., and Goldhaber, M. B., 1977, Recognition of oxidized sulfide minerals as an exploration guide for uranium [abs.]: Am. Assoc. Petroleum Geologists, Rocky Mountain Sec. Ann. Mtg., p. 56.

Rickard, D. T., 1969, The chemistry of iron sulfide formation at low temperatures: Stockholm Contrib. Geology, v. 20, p. 67-95.

Sweeney, R. E., 1972, Pyritization during diagenesis of marine sediments: Univ. Calif., Los Angeles, Ph.D. thesis.